Cancer Cell
Article

Tumor Cells Require Thymidylate Kinase to Prevent dUTP Incorporation during DNA Repair

Chun-Mei Hu,[1] Ming-Tyng Yeh,[4] Ning Tsao,[5] Chih-Wei Chen,[1] Quan-Ze Gao,[2] Chia-Yun Chang,[1] Ming-Hsiang Lee,[5] Jim-Min Fang,[4] Sheh-Yi Sheu,[2,3] Chow-Jaw Lin,[1] Mei-Chun Tseng,[6] Yu-Ju Chen,[6] and Zee-Fen Chang[1,*]
[1]Graduate Institute of Biochemistry and Molecular Biology
[2]Institute of Biomedical Informatics
[3]Department of Life Sciences and Institute of Genome Sciences
National Yang-Ming University, Taipei, 11221 Taiwan
[4]Department of Chemistry, National Taiwan University, Taipei, 10617 Taiwan
[5]Institute of Biochemistry and Molecular Biology, College of Medicine, National Taiwan University, Taipei, 10051 Taiwan
[6]Institute of Chemistry, Academia Sinica, Nankang, Taipei 115, Taiwan
*Correspondence: zfchang@ym.edu.tw
DOI 10.1016/j.ccr.2012.04.038

SUMMARY

The synthesis of dTDP is unique because there is a requirement for thymidylate kinase (TMPK). All other dNDPs including dUDP are directly produced by ribonucleotide reductase (RNR). We report the binding of TMPK and RNR at sites of DNA damage. In tumor cells, when TMPK function is blocked, dUTP is incorporated during DNA double-strand break (DSB) repair. Disrupting RNR recruitment to damage sites or reducing the expression of the R2 subunit of RNR prevents the impairment of DNA repair by TMPK intervention, indicating that RNR contributes to dUTP incorporation during DSB repair. We identified a cell-permeable nontoxic inhibitor of TMPK that sensitizes tumor cells to doxorubicin in vitro and in vivo, suggesting its potential as a therapeutic option.

INTRODUCTION

An important process during DNA repair is the availability of a supply in sufficient amounts of four dNTPs (Niida et al., 2010b). Ribonucleotide reductase (RNR)-mediated reduction directly generates dADP, dGDP, dCDP, and dUDP from their corresponding NDPs (Nordlund and Reichard, 2006). RNR is composed of the R1 and R2 subunits, with the level of R2 being subject to cell cycle regulation (Engström et al., 1985); R2 is often found to be elevated in tumor cells (Jensen et al., 1994; Zhang et al., 2009). It has been reported that R2 overexpression confers oncogenic potential (Fan et al., 1998). An analog of R2, p53R2, can be used to substitute for R2 in the RNR enzyme, and its function is important for DNA repair in quiescent cells (Håkansson et al., 2006; Pontarin et al., 2011). Nucleotide diphosphate kinase converts all dNDPs to dNTPs, including dUTP. Pyrophosphorolysis of dUTP by dUTPase or deamination of dCMP yields dUMP, which can then be converted to dTMP by thymidylate synthase. The action of thymidine kinase (TK) is also able to generate dTMP from thymidine. Thymidylate kinase (TMPK) subsequently catalyzes the formation of dTDP (Reichard, 1988). Thus, dTDP is the only dNDP formation that cannot be directly generated through the action of RNR.

Repair of double-strand breaks (DSBs) is mediated by the homologous recombination (HR), single-strand annealing (SSA), or nonhomologous end-joining (NHEJ) pathways (Hartlerode and Scully, 2009). NHEJ occurs during G1 phase and facilitates the direct ligation of the two DNA ends that are associated with DSBs (Lieber, 2010). Both the SSA and HR pathways involve 5′ resectioning from a DSB site to generate a long 3′ overhang (Mimitou and Symington, 2009). The SSA pathway repairs DSBs between or within linked direct repeats in which the 3′ overhangs are annealed in a way that is dependent on the presence of these repeat sequences in the same DNA duplex, and

Significance

The present study reveals that high levels of RNR at sites of DNA damage in tumor cells without coordination with TMPK seems to lead to dUTP incorporation during repair. Normal cycling cells, which have an intact checkpoint, express low levels of R2 after DNA damage, thereby dispensing with the requirement for TMPK during repair. Conventional cancer chemotherapy by DNA damage is unable to discriminate between tumor cells and rapidly dividing cells in normal tissues, which can often lead to unwanted side effects. This study offers a strategy by which TMPK is targeted as an adjunctive therapy that aims to minimizing side effects.

any unannealed sequences are then deleted followed by ligation to restore the continuous DNA duplex. HR repair at a DSB site produces a long 3′ single strand and employs DNA duplex containing a long homologous sequence as the template for strand exchange and resynthesis, which results in a repair of the DSB (San Filippo et al., 2008). The HR repair process is error free and mainly occurs during late S and G2 phases, when sister chromatids are available as the HR templates. The new synthesis of long strands during HR requires the incorporation of more than 10,000 dNTPs in order to repair a single DSB by strand invasion (Robert et al., 2011). The RNR-mediated supply of dNTPs is thus critical to successful HR repair (Burkhalter et al., 2009; Moss et al., 2010).

Because formation of dTDP specifically requires TMPK functionality, we have hypothesized that blocking TMPK should also reduce the efficiency of DSB repair and sensitize tumor cells to genotoxic insults. Using RNA interference, we have previously shown that TMPK knockdown significantly increases the sensitivity of HCT-116 colon cancer cells to doxorubicin, a topoisomerase II inhibitor that induces DSBs in DNA (Hu and Chang, 2008). In comparison, TS knockdown only sensitizes *p53*-deficient cells to doxorubicin to a limited extent because of complementation of TK-mediated dTMP formation. Importantly, we found that TMPK knockdown does not, on its own, activate DNA damage responses. It thus functions in a way that is quite distinct from that of the antimetabolites used in conventional anticancer therapies, which directly induce genotoxicity (Garg et al., 2010). For example, the thymidylate synthase inhibitors 5-FU and 5-FdUrd block the conversion of dUMP to dTMP, causing dUTP to accumulate and inducing the formation of 5-FdUTP (Longley et al., 2003). DNA polymerases are unable to discriminate between dUTP and dTTP (Bessman et al., 1958), and, therefore, excessive amounts of dUTP and 5-FdUTP are misincorporated into DNA, which triggers DNA damage-induced cell death (Ahmad et al., 1998). Consequently, such antimetabolites are highly toxic to normal cycling cells and potentially may induce the development of secondary tumors.

TMPK-knockdown cells are viable and capable of proliferating (Hu and Chang, 2008). Given the essential function of TMPK during dTDP formation, this suggests that human tumor cells have a TMPK isoform. However, it is hard to understand why TMPK knockdown profoundly affects DNA repair in tumor cells. Unlike TMPK knockdown, blocking RNR by itself induces a DNA damage response and blocks DNA repair (Shao et al., 2006). A recent report has demonstrated that RNR is recruited to sites of DNA damage as a result of an interaction with Tip60 via the C-terminal region of the R1 subunit (Niida et al., 2010a). Disruption of RNR recruitment to sites of DNA damage affects DSB repair in G1-phase cells but not in S-phase cells. The explanation for this is that the low levels of dNTPs in G0/G1-phase cells make the site-specific production of dNTPs by RNR critical to DNA repair (Håkansson et al., 2006). In this study, we have provided evidence linking the involvement of RNR at DNA damage sites to the functional requirement of TMPK for DNA repair in tumor cells. Additionally, we identified a cell-permeable inhibitor of hTMPK. Our results further demonstrate the potential of TMPK inhibitors to be part of mild anticancer therapies.

RESULTS

TMPK Contributes to the Repair of DSBs by Preventing dUTP Incorporation

To assess the role of TMPK in DSB repair, we silenced TMPK expression in U2OS cells harboring a DR-GFP reporter using siRNA and performed HR analysis (Pierce et al., 1999). In the presence of I-SceI endonuclease, which induces DSBs, HR repair generates intact GFP, which gives a fluorescent readout. Using flow cytometry analysis, it was found that TMPK knockdown significantly reduced the efficiency of HR repair, as determined by measuring the GFP-positive fraction (Figure 1A). Cell-cycle analysis showed that TMPK knockdown did not reduce the numbers of U2OS cells in the S and G2/M phases (Figure 1A and Figure S1A, which is available online), which excludes the possibility that TMPK knockdown reduces the number of HR-permissive cells. We also tested the effect of TMPK knockdown on the repair of doxorubicin-induced DNA lesions in MDA-MB231 breast cancer cells. Control and TMPK-knockdown cells were treated with a low dose of doxorubicin (0.1 μM) for 4 hr and then were washed thoroughly with growth medium. Initially, the number of DNA lesions, as indicated by γH2AX focus staining (Mah et al., 2010), was similar in these cells to the control (Figure 1B). After recovery for 24 hr, the number of doxorubicin-induced DNA lesions was reduced in the control cells, indicating that these cells were capable of repairing the DNA damage induced by exposure to low-dose doxorubicin. In contrast, the number of γH2AX foci in the TMPK-knockdown cells was relatively constant and significantly higher than in the control. Moreover, TMPK knockdown on its own had only a slight effect on the growth of MDA-MB231 cells, which contrasted with the marked reduction in cells growth found when cells were exposed to doxorubicin (Figures S1B and S1C). Thus, TMPK would seem to be essential for DNA repair in MDA-MB231 cells when they are exposed to low-dose doxorubicin.

Doxorubicin exposure-induced DSBs are repaired by HR. It is known that HR involves Rad 51 foci, which is where strand invasion takes place during repair (Holthausen et al., 2010). We tested the effect of TMPK knockdown on the formation and resolution of Rad 51 foci following exposure to doxorubicin. The results show that TMPK knockdown did not initially affect Rad51 focus formation. However, after 24 hr, the number of Rad 51 foci was significantly reduced in the control cells but not in TMPK-knockdown cells (Figure 1C). This indicates that TMPK knockdown prevents the repair of recombinogenic lesions. We also examined XRCC1 foci, which are known to be single-strand break-repair (SSBR) markers (Caldecott, 2008). As expected, very few XRCC1 foci were detected in control and TMPK knockdown cells immediately after exposure. At 24 hr after recovery, TMPK knockdown cells showed a marked increase in the number of XRCC1 foci (Figure 1D), which implies that blocking TMPK promotes the presence of DNA single-strand breaks (SSBs) formation during HR.

It is well established that SSBs are generated via the removal of erroneous bases by DNA glycosylases and via apurinic/apyrimidinic endonuclease (APE)-mediated cleavage at the abasic sites (Caldecott, 2008). Uracil DNA glycosylases, such as uracil N-glycosylase (UNG), remove uracil from DNA (Krokan

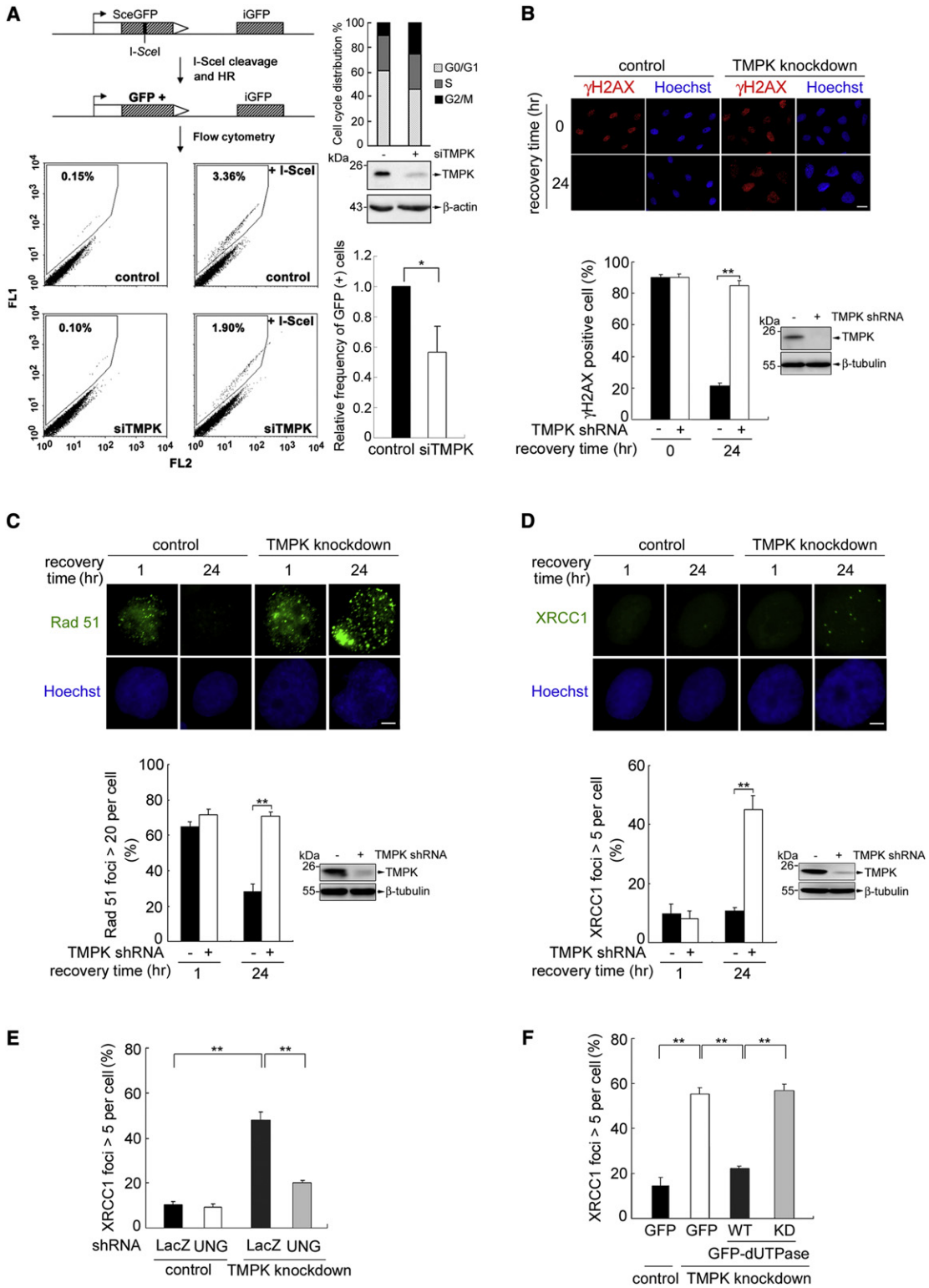

Figure 1. TMPK Knockdown Causes DSB Repair with dUTP Incorporation

(A) Following transfection with TMPK siRNA for 24 hr, U2OS-DR-GFP cells were transfected with pCBA-I-SceI plasmid for 48 hr. The frequency of GFP-positive cells was measured by FACS analysis. In parallel, cells were fixed with PI staining for FACS analysis and harvested for Western blot analysis.

(B–D) MDA-MB231 cells without and with TMPK shRNA stable expression were exposed to doxorubicin (0.1 μM) for 4 hr and then underwent recovery in refreshing medium to give γH2AX foci staining (B) (scale bar, 20 μm), Rad51 foci staining (C) (scale bar, 5 μm), and XRCC1 foci staining (D) (scale bar, 5 μm). Each cell containing γH2AX foci > 10, Rad51 foci > 20, and XRCC1 foci > 5 were counted and expressed as a percentage.

et al., 2002). To test whether the SSBs identified as XRCC1 foci resulted from the misincorporation of uracil, TMPK-knockdown cells were infected with lentiviral shRNA for UNG. After recovery from doxorubicin exposure, it was found that the number of XRCC1 foci was markedly reduced by UNG knockdown (Figure 1E and Figure S1D). To verify the presence of uracil in the genome of the cells after recovery from doxorubicin exposure, we isolated genomic DNA by in vitro UNG incubation and analyzed small molecules released from genomic DNA by mass spectrometric analysis. The mass spectrum showed the presence of uracil signal in the sample from TMPK knockdown but not control cells (Figure S1E). Thus, blocking TMPK promotes SSBs as a result of the presence of uracil in the genome during the repair of doxorubicin-induced DSBs.

We next tested whether the increase in uracil in the genome was a result of dUTP incorporation. Cellular levels of dUTP are primarily controlled by dUTPase, an enzyme responsible for hydrolyzing dUTP to dUMP and pyrophosphate (McIntosh et al., 1992). Wild-type GFP-dUTPase and a catalytically dead mutant form of GFP-dUTPase (Figure S1F) were expressed in TMPK-depleted MDA-MB231 cells. After recovery from doxorubicin exposure, expression of wild-type dUTPase was found to significantly reduce the number of XRCC1 foci in TMPK-knockdown cells compared to cells expressing the catalytically dead dUTPase, which retained a high level of XRCC1 foci (Figure 1F and Figure S1G). Consistently, γH2AX foci were abolished by overexpression of wild-type, but not catalytically dead, dUTPase (Figure S1H). In conclusion, our results show that TMPK is essential for preventing dUTP incorporation during the repair of DSBs.

Repair at Sites of DNA Damage Requires Coordination between RNR and TMPK

It has been estimated that the dUTP/dTTP ratio in cells is normally within the range 0.3% to 3% (Traut, 1994). TMPK-knockdown cells retain more than 60% of the dTTP pool and are able to proliferate albeit a slower rate (Figures S2A and S2B). Presumably, the cellular level of dTTP is still much higher in these cells than the level of dUTP. This prompted us to question why knockdown of TMPK should cause the incorporation of dUTP during DNA repair. To assess the functional requirements for this TMPK during DNA repair, MDA-MB231 breast cancer cells were transfected with pEGFP-TMPK(WT) or pEGFP-TMPK(D15R), a catalytically dead mutant (Figure S2C). Overexpression of TMPK(WT) resulted in an increased rate of disappearance of γH2AX foci after recovery from doxorubicin exposure. In contrast, overexpression of TMPK(D15R) resulted in the persistence of the γH2AX foci (Figure 2A). It should be mentioned that, when we overexpressed TMPK(D15R) in HeLa cells with high transfection efficiency, it was found that the steady-state level of dTTP was unaffected (Figures S2D and S2E). Given that functionality of endogenous TMPK does not seem to be significantly affected by the expression of TMPK(D15R), the inhibitory effect of TMPK(D15R) on DNA repair is thus unlikely to be related to the size of the dTTP pool.

The RNR-mediated reaction yields dUDP, which is converted to dUTP by NDP kinase (Mathews, 2006). TMPK knockdown results in the incorporation of dUTP during DNA repair, and, therefore, we examined the effect on repair of blocking the recruitment of RNR to sites of DNA damage in TMPK-knockdown MDA-MB231 cells. To this end, we overexpressed YFP fused to a 90-amino-acid C-terminal fragment of the R1 subunit (R1C–NLS–YFP), which interferes with the interaction between endogenous RNR and Tip60 that is required for recruitment to sites of damage (Niida et al., 2010a). Remarkably, overexpression of this R1C–NLS–YFP fusion protein abolished the effect of TMPK knockdown on the number of γH2AX foci during recovery from doxorubicin exposure (Figure 2B). The effect of TMPK(D15R) overexpression was also reversed by expression of R1C–NLS–YFP (Figure 2C). Thus, RNR functionality at sites of DNA damage requires functional coordination with TMPK in order to prevent dUTP-mediated lesions from persisting.

In order to determine whether TMPK and RNR are recruited to sites of DNA damage, we used laser microirradiation to damage DNA, and it was found that γH2AX and endogenous TMPK and R2 colocalized along the microirradiated line (Figure 2D). Consistently, R1 was also found colocalized with γH2AX (Figure S2F). In addition, we transfected cells with an expression vector encoding I-PpoI, which introduces specific DSB in chromosome 1 and ribosomal DNA (Flick et al., 1998). This system allows analysis of the recruitment of the repair proteins to specific DSB sites (Berkovich et al., 2007). We cotransfected cells with pFlag-TMPK to allow chromatin immunoprecipitation (ChIP). Quantitative ChIP analysis showed the presence of Flag-TMPK at the I-PpoI cleavage site in chromosome 1 but not at the c-*fos* promoter region. γH2AX and the R2 subunit of RNR were also present at the I-PpoI cleavage site, but histone 3 (H3) occupancy was not affected by I-PpoI cleavage (Figure 2E). Similar results were observed for ribosomal DNA compared to the control gene GAPDH using ChIP analysis, which additionally showed that the association of UBF, a specific rDNA-binding protein, was not affected by I-PpoI cleavage (Figure S2G). These results suggest that TMPK and RNR bind to sites of DNA damage where they coordinate the site-specific production of balanced amounts of the four dNTPs needed for repair.

High Levels of R2 Expression after DNA Damage Are a Determinant of Tumor Cells that Require TMPK for Repair

We further tested the requirement of TMPK for DNA repair in another breast cancer cell line, MCF-7, as well as in nontumorigenic cycling mammary H184B5F5/M10 and MCF10A cells. In

(E) Cells were infected with lentivirus of LacZ or UNG shRNA for 8 hr. After another 36 hr, cells were exposed to doxorubicin (0.1 μM) for 4 hr and allowed to recover in fresh medium for 24 hr before fixation and XRCC1 foci staining (scale bar, 5 μm). The inset indicates the Western blot data of UNG, TMPK, and GAPDH. For each experiment in (B–E), 100 cells were counted.

(F) Cells were transfected with wild-type and catalytic-dead dUTPase expression plasmids. After overnight incubation, the cells were treated with doxorubicin and recovered for XRCC1 staining as described in (E). The numbers of GFP-positive cells with > 5 XRCC1 foci per cells are shown in the upper panel. For each experiment, 100 GFP-positive cells were counted. All error bars represent SD (n = 3).

See also Figure S1.

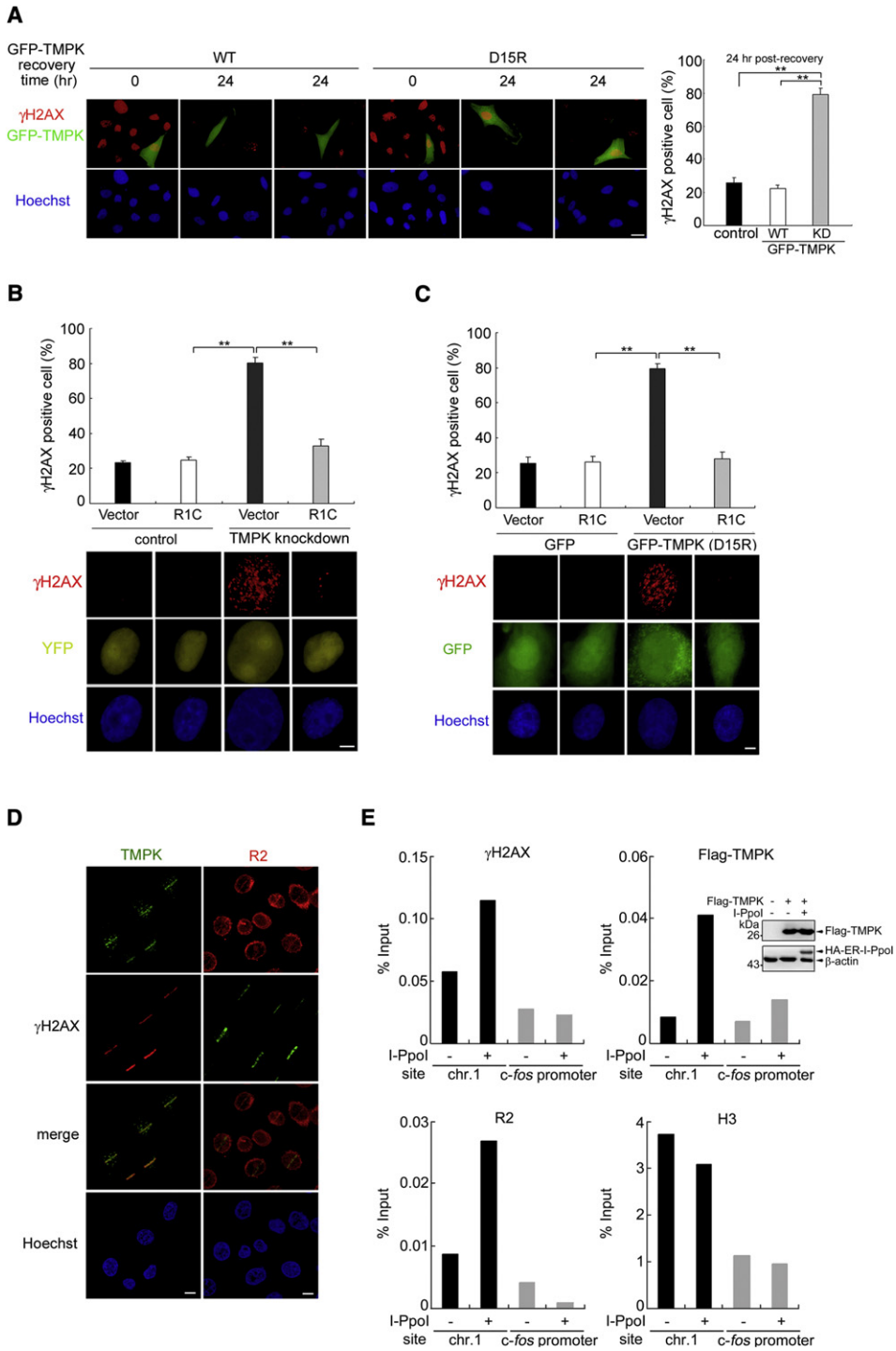

Figure 2. Coordination of TMPK with RNR at Sites of DNA Damage during Repair

(A) MDA-MB231 cells were transfected with pEGFP-TMPK (WT or D15R) followed by doxorubicin exposure and recovered as described in the legend to Figure 1B. Cells were fixed for γH2AX staining (scale bar, 20 μm). For each experiment, 100 GFP-positive cells were counted.

(B) Cells without and with stable TMPK shRNA expression were transfected with pCMV2-YFP-Nuc (vector) or pCMV2-YFP-Nuc-R1C (R1C) plasmid (scale bar, 5 μm).

(C) Cells were transfected with pEGFP-TMPK (D15R) in combination with pCMV2-YFP-Nuc-R1C (R1C) plasmid as indicated. Following doxorubicin exposure and recovery for 24 hr, these cells were analyzed by γH2AX foci staining (scale bar, 10 μm). For each experiment, 100 YFP- or GFP-positive cells were counted. All error bars represent SD (n = 3).

(D) HeLa cells were plated on glasses-like dishes for laser-micro-irradiation. After recovery for 5 min, cells were fixed for γH2AX, TMPK, and R2 immunofluorescence staining (scale bar, 10 μm).

a similar manner to that which occurred with MDA-MB231 cells, TMPK knockdown caused doxorubicin-induced γH2AX foci to persist in MCF-7 cells. In contrast, DNA repair was unaffected by TMPK knockdown in H184B5F5/M10 and MCF10A cells (Figure 3A). We compared expression levels of R2, p53R2, TMPK, and dUTPase during recovery from DNA damage in MDA-MB231, MCF-7, H184B5F5/M10, and MCF10A cells (Figure 3B). Expression of the R2 subunit of RNR and dUTPase was much higher in MCF-7 cells than in H184B5F5/M10 and MCF10A cells. In MDA-MB231 cells, the levels of R2 and dUTPase increased concomitantly between 12 and 48 hr after doxorubicin exposure, which contrasted with their continuous decline in H184B5F5/M10 and MCF10A cells. Expression of p53R2 was very low in MDA-MB231 cells because of the p53 functional deficiency. In MCF-7, H184B5F5/M10, and MCF10A cells, the expression of p53R2 increased during recovery from doxorubicin exposure (between 24 and 48 hr). Flow cytometry analysis demonstrated that the G0/G1-phase cell populations in H184B5F5/M10 and MCF10A cells were 2–3-fold higher than those in MDA-MB231 and MCF-7 cells during recovery from DNA damage (Figure 3C). The larger S and G2/M cell populations in MDA-MB231 and MCF-7 cells during recovery indicate a lower stringency of checkpoint control in response to genome insults in these cells. It has been shown that G2/M synchronization by nocodazole treatment promotes HR (Katada et al., 2012). We further treated H184B5F5/M10 cells with nocodazole overnight to block mitotic progression, which increased the G2/M cell population as confirmed by flow cytometry (Figure 3D and Figure S3A). It was noted that the level of R2 was decreased in nocodazole-treated cells (Figure 3D) probably because of mitotic degradation (Chabes et al., 2003). After washing out nocodazole, the released cells at 24 hr had less than 20% of G2/M population (Figure S3). Very differently, the nocodazole released cells after doxorubicin exposure, and recovery at 24 hr still contained more than 50% G2/M population. Under this situation, these H184B5F5/M10 cells with increased G2/M cell numbers were still insensitive to TMPK knockdown during DNA repair (Figure 3E). Therefore, the lack of TMPK sensitivity in DNA repair in H184B5F5/M10 cells is unlikely due to less HR-permissive cells after doxorubicin exposure. We also compared the cell growth rates of these four cell lines. Under our experimental conditions, H184B5F5/M10 and MCF10A cells proliferated more rapidly than did MDA-MB231 and MCF-7 cells (Figure S3B). These results indicate that the differences in sensitivity to TMPK knockdown in the context of DNA repair efficiency are not correlated with the proliferation rate of the cell lines nor are they determined by the cell cycle distribution.

Given that RNR at sites of DNA damage contributes to the incorporation of dUTP in TMPK-knockdown MDA-MB231 cells, we tested whether elevation of R2 levels in tumor cells is a major factor determining the requirement for TMPK during DNA repair. MCF-7 cells express high levels of R2 and contain p53R2 at a level similar to that found in H184B5F5/M10 and MCF10A cells. In this context, we reduced the R2 level in MCF-7 cells to a level that was similar to that found in H184B5F5/M10 cells by transfection with siRNA and then exposed the cells to doxorubicin (Figure 4A). Flow cytometric analysis showed that a reduction in R2 levels by siRNA transfection alone or in combination with TMPK knockdown did not decrease the S/G2 cell population significantly (Figure 4B and Figure S4A). At 24 hr after recovery, γH2AX foci were still present in cells transfected with either R2 siRNA alone or R2 and TMPK siRNAs (data not shown). However, at 36 hr after recovery, it was found that a reduction in R2 expression rescued DNA repair in TMPK-knockdown MCF-7 cells (Figures 4C and 4D). Therefore, it would seem that the level of R2 is able to determine whether TMPK knockdown affects DNA repair.

We next selected a MCF10A cell clone with constitutive elevation of R2 expression using a lentiviral vector of mCherry-R2. This cell line was then subjected to TMPK knockdown and DNA repair analysis (Figure 4E). The results showed that overexpression of R2 in combination with TMPK-knockdown caused Rad 51 foci to persist at 24 hr after recovery in MCF10A cells (Figure 4F and Figure S4B) and also promoted XRCC1 foci formation (Figure S4C). As a consequence of these changes, such cells remained γH2AX positive (Figure 4G). The cell-cycle analysis of these cells showed that constitutive elevation of R2 expression did not increase S/G2 cell population (Figure S4D). Thus, elevation of R2 expression renders DNA repair in MCF10A cells sensitive to TMPK knockdown without altering cell-cycle distribution. Taken together, the above results demonstrate that an increase in the level of R2 and the recruitment of RNR to sites of DNA damage are the key factors that make TMPK a critical factor for DNA repair in tumor cells. In other words, increased RNR activity at sites of DNA damage in tumor cells needs to be functionally coordinated with the presence of TMPK to prevent dUTP incorporation.

Screening and Characterization of YMU1 as an hTMPK Inhibitor

On the basis of the fact that there is a specific functional requirement for TMPK during DNA repair in tumor cells that have elevated levels of R2 expression, we next searched for inhibitors of hTMPK that might be useful as an approach to selectively sensitizing tumor cells to doxorubicin. Using a luciferase-coupled TMPK assay (Hu and Chang, 2010) in which the inhibition of TMPK leaves more ATP available for the generation of luminescence by luciferase (Figure 5A), we screened a library of 21,120 small molecules and identified one highly potent compound, YMU1, the structure of which is shown in Figure 5B. An enzymatic assay confirmed that YMU1 is an hTMPK inhibitor with an IC_{50} of 0.61 ± 0.02 μM (Figure 5C) and that the compound has no inhibitory effect on the activity of purified thymidine kinase 1 (TK1) (Figure 5D). To investigate the structure-activity relationship, two fragments of YMU1 (D3 and D6), one isomer

(E) HEK293T cells were transfected with HA-ER-I-PpoI or empty vector together with pFlag-TMPK. After 18 hr, cells were collected and used for qChIP analysis with the indicated antibody using a primer pair adjacent to the I-PpoI cleavage site (280 bp 5′ to the I-PpoI cut site) in chromosome 1. The c-*fos* promoter serves as a genomic DNA control because it has no I-PpoI site. Data were normalized by IgG control and calculated relative to total input (percentage) from two independent experiments.
See also Figure S2.

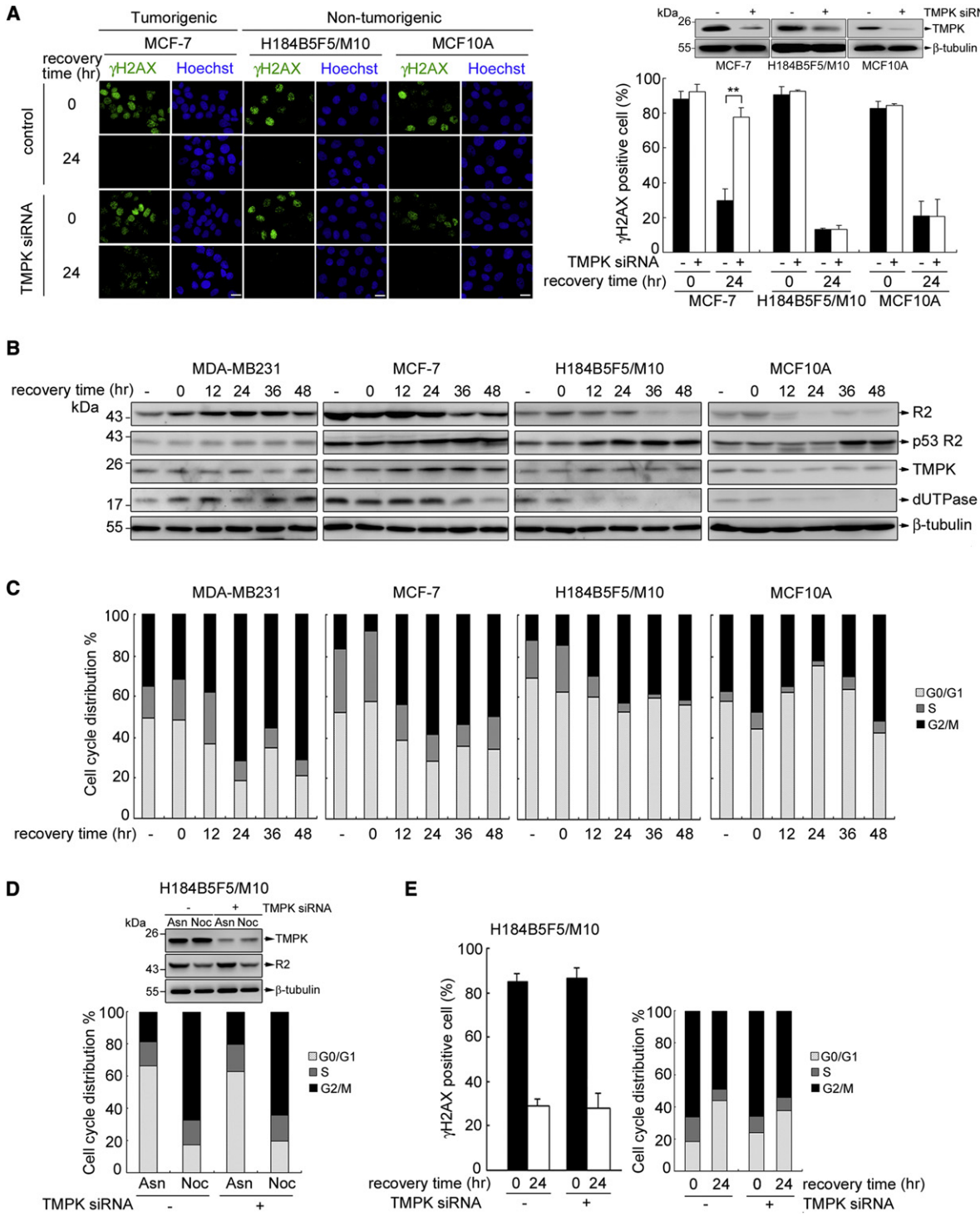

Figure 3. Correlation of the Cellular Level of R2 with the Requirement for TMPK during DNA Repair

(A) MCF-7, H184B5F5/M10, and MCF-10A cells were transfected with TMPK siRNA. These cells were exposed to doxorubicin and recovered for γH2AX foci staining (scale bar, 20 μm), as described in the legend to Figure 1B. For each experiment, 100 cells were counted.

(B and C) Cells were exposed to doxorubicin and then underwent recovery. Cells were harvested at the indicated time points for Western blot (B) and flow cytometry (C) analysis.

(D and E) H184B5F5/M10 cells were transfected with TMPK siRNA for 36 hr and then treated with 500 ng/ml of nocodazole overnight. (D) A proportion of cells were harvested for Western blot and FACS analysis. The rest of cells were exposed to doxorubicin (0.2 μM) for 2 hr and allowed to recover with fresh medium. (E) At the indicated time of recovery, cells were fixed for γH2AX foci staining and FACS analysis. For each experiment, 200 cells were counted.

See also Figure S3.

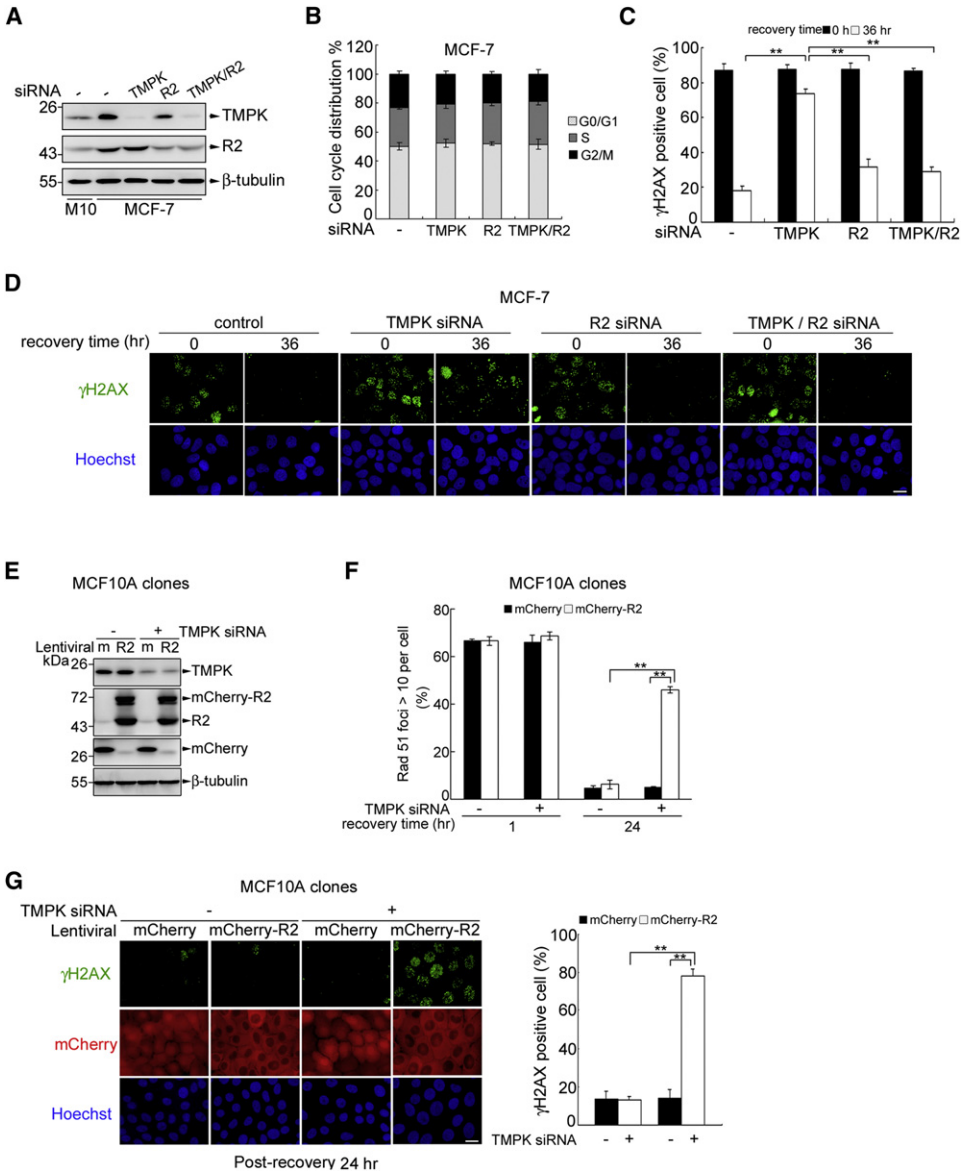

Figure 4. Effect of R2 Expression Level on DNA Repair in Response to TMPK Knockdown

(A and B) MCF-7 cells were transfected with siRNA of TMPK, R2, or TMPK/R2 for 36 hr. A proportion of cells were harvested for Western blot (A) and FACS (B) analysis. The rest of cells were exposed to doxorubicin (0.1 μM) for 4 hr.

(C and D) Cells at the indicated time points were analyzed by γH2AX foci staining, and 150 cells were counted to indicate the percentage of γH2AX foci-positive cells, and representative images are shown (D) (scale bar, 20 μm).

(E–G) MCF10A clones stably expressing mCherry or mCherry-R2 were selected and transfected with TMPK siRNA for 36 hr. (E) Western blot analysis of the cells. (F and G) After exposure to doxorubicin and recovery at indicated time, cells were fixed for Rad 51 (F) and γH2AX foci staining (G) (scale bar, 20 μm). For each experiment in (F) and (G), more than 150 cells were counted. All error bars represent SD (n = 3).

See also Figure S4.

of YMU1 (D7), and a benzeneisothiazolone derivative of YMU1 (D8) were synthesized (Figure 5B). Neither D6 (the piperazine fragment of YMU1) nor D7 (the O-alkylation isomer of YMU1) showed any inhibition of hTMPK, whereas D3 (the pyridinoisothiazolone fragment of YMU1) exhibited weak inhibitory activity. Interestingly and in contrast to the above three compounds, the benzeneisothiazolone derivative D8 also displayed considerable inhibitory activity.

The mode of inhibition of YMU1 was determined by preincubating different concentrations of YMU1 with purified hTMPK protein and measuring the initial velocity in a conventional TMPK assay. The K_m and V_{max} values were determined by nonlinear regression analysis and are summarized in Table 1. Preincubation with YMU1 reduced the V_{max} of hTMPK in a concentration-dependent manner while increasing the *K*m for ATP without significantly affecting the *K*m for TMP. The inhibition

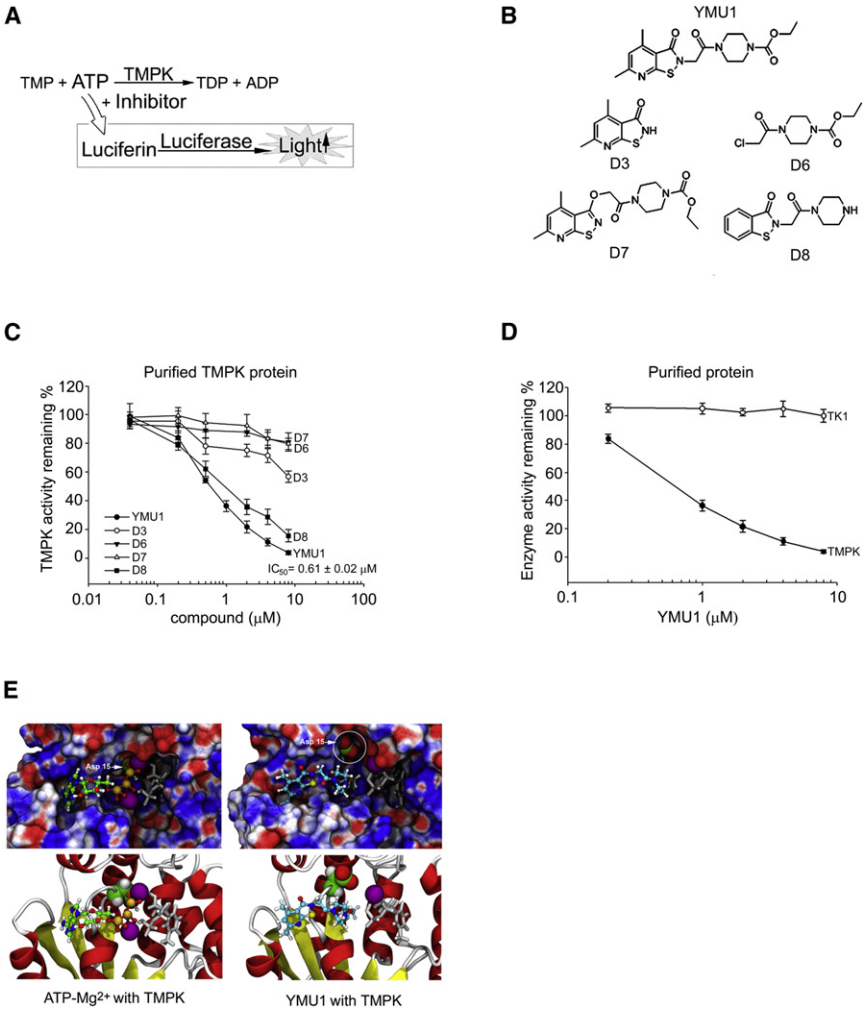

Figure 5. Identification of an hTMPK Inhibitor

(A) A screen for hTMPK inhibitors by luciferase-coupled assay.

(B) The chemical structures of YMU1 and related molecules. The chemical synthesis scheme of YMU1 and related compounds is presented in Supplemental Experimental Procedures.

(C) Effect of YMU1 and derivative compounds on hTMPK inhibition. Activity analysis of purified hTMPK protein (0.5 μg) after 10 min of preincubation with compounds using luciferase-coupled TMPK analysis.

(D) Activity of purified TMPK (0.5 μg) and GST-hTK1 protein (5 μg) that had been preincubated with YMU1 for 10 min prior to the activity assay. All error bars represent SD (n = 4).

(E) Molecular models of the TMPK-YMU1 complex. Left panel: TMPK/ATP/Mg^{2+}; right panel: TMPK/YMU1. The TMPK is represented as surface electrostatic potential (upper) and a structural ribbon (lower). ATP and YMU1 are shown as green and blue stick models, respectively, with colored atoms (O, red; S, yellow; P, orange). TMP is shown as a white backbone and Mg^{2+} is shown in purple. The arrow indicates the position of Asp15.

See also Figure S5.

constant (K_i) was determined by kinetic analysis to be 0.22 ± 0.03 μM (Table 1). Molecular docking studies were performed to analyze the mechanism of inhibition of TMPK by YMU1. The results of the kinetic studies suggest that YMU1 probably affects the ATP-binding pocket of TMPK. Using the crystal structure of TMPK with TMP and Mg^{+2}, it was possible to dock YMU1 into the ATP pocket. During this docking complex, YMU1 prevents one Mg^{+2} ion from interacting with the Asp15 residue in the catalytic domain (Figure 5E). Because a mutation of Asp15 to Arg is known to abrogate TMPK catalytic function, it is possible that preincubation of TMPK with YMU1 hinders the functionality of the Mg^{+2} ion pointing toward the catalytic Asp15 residue in the ATP pocket, thereby reducing catalytic efficiency. The docking of D3, D6, and D7 at these sites was found to not prevent Asp15 from interacting with Mg^{+2} and therefore suggests why these compounds do not inhibit TMPK.

YMU1 reduced cellular dTTP levels by about 30%–40% (Figure S5). Transfection of cells with siRNA to suppress TMPK expression reduced the size of the dTTP pool to a similar extent. YMU1 treatment did not cause any further reduction of the dTTP pool in TMPK-knockdown cells. The levels of dATP, dCTP, and dGTP were unaltered in both YMU1-treated and TMPK-knockdown cells (Figure S5). These results indicate that YMU1 specifically reduces dTTP level and that the ability of YMU1 to reduce dTTP level is dependent on the presence of TMPK in the cells.

YMU1 Is Not Toxic to the Genome and, Similar to TMPK Silencing, Impairs DSB Repair

Inhibition of TS by FdUrd causes genome toxicity (Longley et al., 2003). Given the shared role of TMPK and TS in dTTP synthesis, we next compared the effects of blocking TMPK and TS on the induction of DNA damage of either shRNA interference or inhibitor treatment. As indicated by γH2AX staining, TS silencing and FdUrd treatment induced severe DNA damage, whereas TMPK silencing and YMU1 treatment did not (Figure 6A). We also compared the effects of YMU1 and FdUrd on the viability of non-tumorigenic H184B5F5/M10 and MCF10A mammary cycling cells and MCF-7 and HCT-116 $p53^{-/-}$ tumor cells. A colony assay indicated that FdUrd, but not YMU1, caused cell death in all of these cells (Figure 6B). Therefore, unlike blocking TS, targeting TMPK does not, on its own, cause genome toxicity or cytotoxicity. We also performed MTS assays using human primary bone marrow mesenchymal stem cells (HBMSC), renal cortical epithelial cells (HRCE), mammary epithelial cells (HMEC), and breast tumor MDA-MB231 cells and found that YMU1 had very little effect on cell growth (Figure S6A).

We next examined the effect of YMU1 on the repair of doxorubicin-induced DNA lesions in MDA-MB231 and H184B5F5/M10 cells after recovery from low-dose doxorubicin treatment. Notably, in H184B5F5/M10 cells, YMU1 treatment did not affect the numbers of DNA lesions formed, as determined by γH2AX focus staining. Similar to TMPK knockdown, pretreatment with

Table 1. Effect of YMU1 on the Kinetic Parameters of Purified Human Thymidylate Kinase

YMU1 compound (μM)	*K*m for TMP (μM)	*V*max (nmol/min/mg)	*K*i (μM)
0	28.7 ± 2.4	376.6 ± 14.5	0.22 ± 0.03
0.125	26.5 ± 2.8	258.9 ± 12.4	
0.25	27.5 ± 4.0	180.6 ± 11.8	
0.5	28.0 ± 4.3	91.8 ± 6.4	
YMU1 compound (μM)	*K*m for ATP (μM)	*V*max (nmol/min/mg)	*K*i (μM)
0	25.7 ± 2.4	367.2 ± 9.4	0.18 ± 0.06
0.25	29.5 ± 5.6	212.0 ± 10.3	
0.5	41.2 ± 7.4	94.8 ± 6.9	
1	43.8 ± 3.3	55.7 ± 1.3	

For the *K*i value determination, YMU1 at the indicated concentration was preincubated with 0.5 μg of purified hTMPK protein for 10 min, and the initial velocity of the TMPK reaction was measured at different concentrations of TMP (2–200 μM) in the presence of ATP (1 mM) or at different concentrations of ATP (5–1000 μM) in the presence of TMP (200 μM) using a NADH-coupled TMPK assay. Data represent mean ± SD, n = 4. Data obtained from the nonlinear regression analysis were used to calculate the *K*m and *V*max. The *K*i value of YMU1 for hTMPK was calculated from the equation of $K_i = [I] / (V_{max} / V_{max}' - 1)$, where [I] and *V*max' are the YMU1 compound concentration and maximal velocity in the presence of YMU1, respectively. The *K*i value represents a mean value derived from three different YMU1 concentrations.

YMU1 caused over 70% of the MDA-MB231 cells to remain γH2AX positive at 48 hr after doxorubicin exposure (Figure 6C) but did not affect cell-cycle progression during recovery (Figure S6B). Comet assay analysis further confirmed that YMU1 treatment impaired DNA repair in MDA-MB231 cells exposed to doxorubicin (Figure S6C). Overexpression of GFP-TMPK rendered MDA-MB231 cells resistant to the YMU1-mediated persistence of DNA lesions, supporting the idea that YMU1 exerts its effect by targeting TMPK (Figure 6D). Overexpression of TMPK(WT) in YMU1-treated HeLa cells with high transfection efficiency restored the level of dTTP (Figure 6E). Similar to siRNA knockdown, YMU1 treatment also led to the persistence of Rad 51 foci and an increase in XRCC1 focus formation that was abolished by UNG depletion (Figures 6F–6H). The inhibitory effect of YMU1 on DNA repair was reversed by overexpression of either dUTPase or a 90-amino-acid C-terminal fragment of the R1 subunit of RNR (Figures 6I and 6J), which confirms that the effect of YMU1 on repair toxicity is dependent on the amount of dUTP present at damage sites and recruitment of RNR to the damage sites. Furthermore, YMU did not inhibit dUTPase in vitro (Figure S6D).

YMU1 Sensitizes Malignant Tumor Cells to Doxorubicin In Vitro and In Vivo

Next, various human cancer cell lines were treated with YMU1, the D6 compound, or the D7 compound for 72 hr to test the potential of TMPK inhibition in relation to doxorubicin sensitization. After exposure to different concentration of doxorubicin for 4 hr, cells were subjected to viability analysis, and the IC_{50} value for doxorubicin for each cell line was determined (Figure 7A). YMU1 treatment increased doxorubicin sensitivity in HT-29, HCT-116 $p53^{+/+}$, HCT-116 $p53^{-/-}$, H1299, CL1-0, U2OS, MDA-MB231, MDA-MB468, and SaoS2 cells by 3–35-fold. Two HR defective cell lines, HCC1937 and Capan1 deficient in BRCA1 and 2 (Nagaraju and Scully, 2007; Powell and Kachnic, 2003), were not responsive to YMU1 treatment. YMU1 had little effect on the doxorubicin IC_{50} of mammary cycling H184B5F5/M10 and MCF10A cells, IMR-90 embryonic lung fibroblasts, and primary HMEC and HRCE. The inactive compounds D6 and D7 shown in Figures 5B and 5C did not cause doxorubicin sensitization in any of these cell lines. Western blot analysis indicated that all tumor cells that were sensitized by YMU1 treatment showed elevated levels of R2 expression after doxorubicin exposure (Figure 7B). A colony assay further showed that YMU1 markedly enhanced the lethal effects of doxorubicin (0.1 μM) in HCT-116 and MCF-7 cells (Figure 7C). TMPK knockdown was unable to further sensitize YMU-treated MDA-MB231 cells to doxorubicin (Figure S7A), suggesting that the specificity of YMU1 in terms of doxorubicin sensitization is related to the drug targeting TMPK. Overexpression of wild-type dUTPase prevented YMU1/doxorubicin-induced apoptosis, as revealed by reduced Annexin V staining (Figure S7B).

We also used an in vivo xenograft model using HCT-116 $p53^{-/-}$ cells inoculated into nude mice to examine the effect of YMU1 as an adjuvant on sensitization to low-dose doxorubicin treatment. Tumor growth rates in mice treated with either doxorubicin alone or YMU1 alone were similar to those in control animals. In contrast, the growth of tumors was much slower in the YMU1/doxorubicin double-treated mice (Figure 7D). Two weeks after the last injections were administered, mice were sacrificed, and tumor weights measured. We observed excellent tumor suppression in the YMU1/doxorubicin double-treated mice, with an average tumor size that was 25% of the control mice (Figure 7E). Under these experimental conditions, the tumor sizes remained similar in mice treated with doxorubicin alone or YMU1 alone. In agreement with these tumor-growth data, the tumor proliferation index, determined by measuring Ki 67 immunostaining, was clearly reduced in the nude mice treated with both YMU1 and doxorubicin (Figure 7F). We also treated mice bearing larger tumors of various different sizes formed by HCT-116 $p53^{+/+}$ cell implantation. The results consistently showed that the joint therapy of YMU1 with doxorubicin significantly suppressed tumor growth (Figure S7C). Furthermore, Balb/c mice were treated with YMU1 for 4 weeks, using a 2-fold higher dose regimen than that used in the tumor xenograft study. YMU1 treatment did not alter mouse body weight over the course of 4 weeks. Additionally, the weights of various organs (heart, liver, spleen, lungs, and kidneys) and the results of hematological analyses of the YMU1-treated mice were similar to those of the control mice (Table S1). Taken together, these results indicate that, on its own, YMU1 seems to produce no obvious toxic effects in normal mice and that, in conjunction with low-dose doxorubicin, YMU1 suppresses tumor growth in mice.

DISCUSSION

In this study, we provide insights into the functional requirement of TMPK for DNA repair in tumor cells. Our results suggest that RNR at the sites of DNA damage may be responsible for the

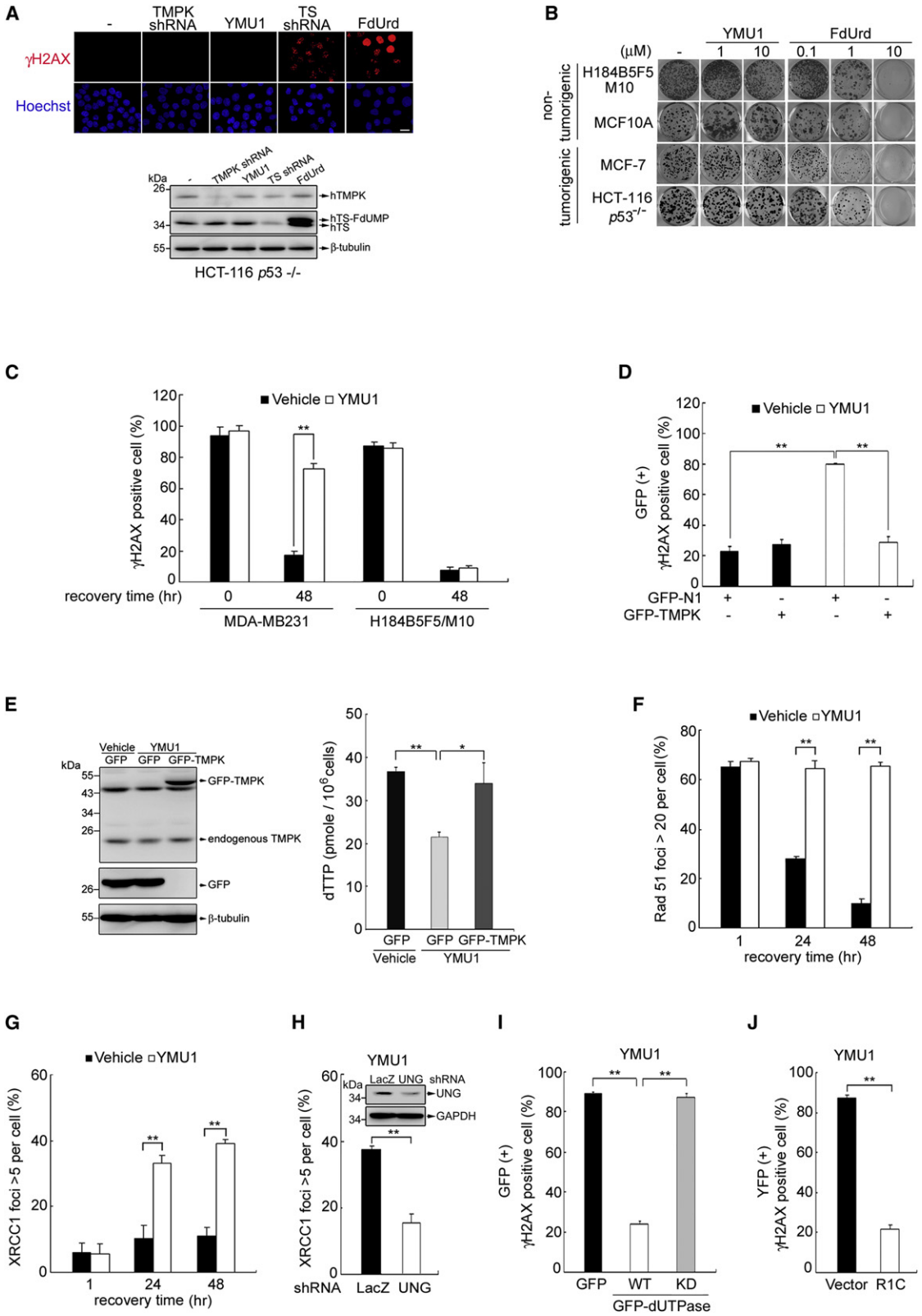

Figure 6. Effect of YMU1 on Genomic Toxicity and DNA Repair

(A) HCT-116 *p53*$^{-/-}$ cells were infected with lentivirus of TMPK or TS shRNA. In parallel, cells were treated with YMU1 (2 μM) for 2 days, or 5-fluoro-2′deoxyuridine (FdUrd, 2 μM) for 1 day. These cells were fixed for γH2AX foci staining (scale bar, 20 μm) and Western blot analysis.

site-specific production of dUTP. Theoretically, the formation of dUMP by dUTPase and the TS-mediated reaction that converts dUMP to dTMP should limit the amount of cellular dUTP. However, blocking TMPK function causes the incorporation of dUTP during DNA repair in tumor cells, a response that is dependent on the recruitment of RNR to the sites of damage; these findings reveal the physiological complexity of the site-specific production of dUTP by the RNR. We propose that blocking TMPK reduces the rate of dTTP formation at sites of damage, whereas increased RNR function is able to increase site-specific dUTP production. Because HR requires the incorporation of more than 10,000 dNTPs to repair each DSB, the probability of dUTP incorporation is increased, which leads to persistent lesions. Given that RNR activity is elevated in tumor cells after DNA damage, blocking TMPK function sensitizes tumor cells to doxorubicin (Figure 7G). In agreement with our hypothesis, we found that HR-defective tumor cells were not responsive to the blocking of TMPK during the repair of doxorubicin-induced lesions.

Expression of the R2 subunit of RNR and dUTPase is cell-cycle regulated, peaking during the S and G2/M phases (Ladner and Caradonna, 1997; Nordlund and Reichard, 2006). Malignant tumor cells have cell-cycle checkpoint defects (Kastan and Bartek, 2004). Therefore, tumor cells recovering from low dosage of DNA damage have greater S-phase and G2/M-phase populations, during which HR-mediated DNA repair can take place with an increase of R2 expression, and this has a requirement for TMPK functionality. In contrast, the S-phase population is reduced in nontumorigenic cycling cells during recovery from DNA damage because of the presence of an intact checkpoint control. As a result, these cycling cells express even lower amounts of R2, which may further limit dUDP formation.

Because nontumorigenic cycling cells after DNA damage have fewer S/G2 cells, the question is whether the R2 level or cell-cycle phase permissive for HR determines the requirement for TMPK during DNA repair. In this study, we provide evidence that the manipulation of increasing the G2/M-phase cell does not make nontumorigenic cycling cells sensitive to TMPK knockdown during DNA repair, whereas enforced expression of R2 does. Because MCF10A and H184B5F5/M10 nontumorigenic cells do not grow any slower than MDA-MB231 and MCF7 cells, these results led us to conclude that the elevation of R2 after DNA damage is a key factor affecting the requirement for TMPK in the repair of doxorubicin-induced DNA lesions. In view of the elevation of R2 expression in tumor cells being associated with their continued S/G2 progression after low dosage of DNA damage, checkpoint defects in tumor cells would seem to be closely related to the requirement for TMPK during DNA repair. If so, it is possible that patients with tumor containing a high R2/TMPK ratio should be more responsive to doxorubicin therapy. Because expression levels of R2 and TMPK are controlled by transcription and proteolysis, it is necessary to generate new TMPK antibody applicable for immunohistochemical analysis. In addition, such an analysis in tumor samples from patients before chemotherapy may not be informative for predicting response, because some tumors do not express high levels of R2 until with genotoxic treatment.

Notably, normal cycling cells contain appreciable levels of the p53R2 subunit, which is capable of forming functional RNR at sites of DNA damage. This opens up the question as to why DNA repair in normal cycling cells is not affected by TMPK knockdown. One plausible explanation is that R2 has a 4.7-fold higher binding affinity for R1 than does p53R2 (Shao et al., 2004). It is possible that the low affinity of p53R2 for the R1 subunit reduces the efficiency of the RNR and minimizes the site-specific production of dUTP in normal cycling cells. This would thereby abolish the functional requirement for TMPK at sites of DNA damage repair. Indeed, enforced expression of R2 in normal cycling cells causes an impairment of DNA repair in TMPK knockdown cells, which supports our conclusion that DNA repair toxicity induced by TMPK knockdown is linked to an increase in RNR functionality. Expression of R2 and p53R2 has been found to be upregulated in many types of cancer cells in patients (Yanamoto et al., 2003; Zhang et al., 2009). Tumors form in transgenic mice overexpressing R2 or p53R2 in the lungs (Xu et al., 2008). Whether the side effects of dUTP formation by RNR at sites of DNA damage are related to their oncogenic potential remains to be investigated. Nevertheless, it is noteworthy that p53R2 predicts better survival in patients with colorectal cancer, whereas R2 level is correlated with increased aggressiveness of tumors (Liu et al., 2011). Expression of an RNR mutant defective in dATP feedback inhibition in yeast causes elevation of dNTP, which is accompanied by an inhibition of cell-cycle progression and the DNA damage

(B) H184B5F5/M10 cells were seeded at 5,000 cells/100 mm-dish. MCF10A, MCF-7, and HCT-116 $p53^{-/-}$ cells were seeded onto 6-well plates at the density of 600 cells/well. Following an overnight incubation, the cells were treated with YMU1 or FdUrd at the indicated concentration twice a week. After 14 days, colonies were fixed and stained by crystal violet.
(C) Cells were pretreated with vehicle or YMU1 (2 μM) for 72 hr and then exposed to doxorubicin (0.1 μM) for 4 hr. After replacing with fresh medium, the cells were fixed for γH2AX foci staining at the indicated time.
(D) MDA-MB231 cells after vehicle or YMU1 (2 μM) treatment for 48 hr were transfected with pEGFP-N1or pEGFP-TMPK plasmid. After incubation overnight, the cells were exposed to doxorubicin and recovered as described above. At 24 hr, the cells were analyzed by γH2AX foci staining.
(E) HeLa cells were treated with vehicle or YMU1 (10 μM) for 24 hr and transfected with GFP or GFP-TMPK (WT). After 48 hr, cells were harvested for Western blot and dTTP level analysis.
(F and G) MDA-MB231 cells pretreated with vehicle or YMU1 (2 μM) for 72 hr, then exposed to doxorubicin, followed by recovery as described above for Rad51 foci (F) and XRCC1 foci (G) staining.
(H) Cells were infected with lentivirus carrying LacZ or UNG shRNA for 8 hr. After exposure to doxorubicin and recovery for 24 hr, the cells were fixed for XRCC1 foci staining. Inset indicates the levels of UNG protein by Western blotting analysis. For each experiment in (C–G), more than 100 of the cells were counted.
(I and J) MDA-MB231 cells pretreated with YMU1 (2 μM) for 48 hr were transfected with indicated plasmid or shRNA. After overnight incubation, the cells were exposed to doxorubicin and then underwent recovery as described above. After 24 hr, the cells were analyzed by γH2AX foci staining. For each experiment, 100 GFP-positive or YFP-positive cells were counted. Error bars represent SD (n = 3).
See also Figure S6.

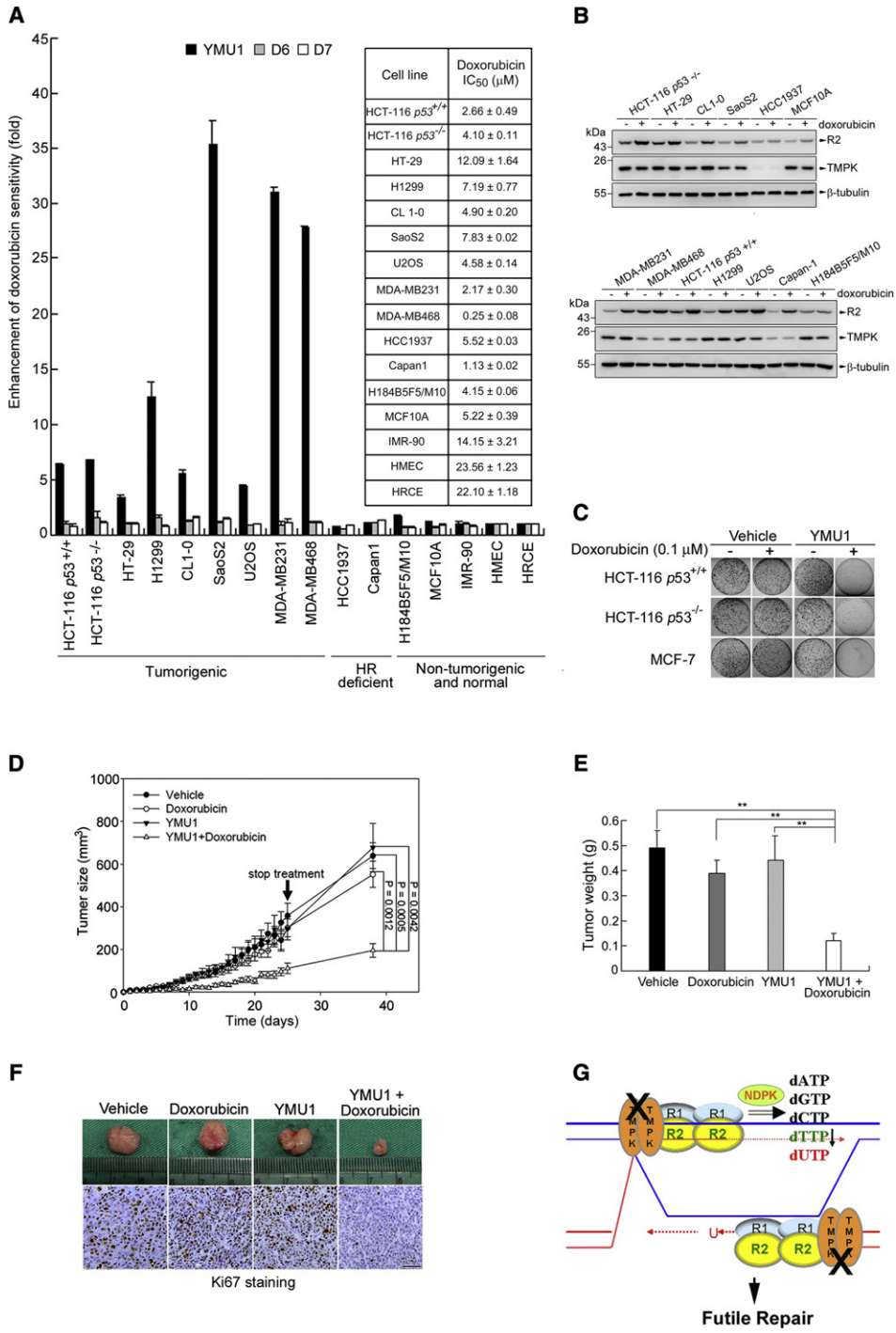

Figure 7. In Vitro and In Vivo Effect of YMU1 on Doxorubicin Sensitization

(A) Various cell lines were pretreated with vehicle, YMU1, D6, or D7 for 3 days. D6 and D7 are inactive molecules shown in Figure 5B. The cells were exposed to different concentration of doxorubicin for 4 hr. After 48 hr of recovery from doxorubicin exposure, the cells were subjected to MTS assay in quadruplicate, and the IC_{50} for doxorubicin was determined. The enhancement (fold) of doxorubicin sensitivity for each cell line was calculated. Error bars represent SD (n = 3). The inset indicates the IC_{50} value of doxorubicin for each cell line.

(B) Cells (1×10^6) were plated in a 60 mm dish. After an overnight incubation, cells were exposed to without or with doxorubicin (0.5 μM) for 4 hr and allowed to recover in fresh medium for 16 hr. The cells were then harvested for western blot analysis.

(C) After treatment with vehicle or YMU1 for 72 hr, the cells were exposed to 0.1 μM doxorubicin for 4 hr and then seeded onto a 100 mm-dish at 5,000 cells/dish. Following an overnight incubation, the cells were refreshed with growth medium for 14 days of incubation for colony formation.

(D) HCT-116 $p53^{-/-}$ cells were subcutaneously implanted in the right flank of Balb/c nude mice. The arrow indicated the time when drug treatment was stopped. The tumor volume was determined.

checkpoint (Chabes and Stillman, 2007). Whether this phenomenon involves dUTP formation is also worthy of investigation.

Our findings suggest that a tumor context with checkpoint defect to allow an R2 elevation after DNA damage makes TMPK an Achilles heel for doxorubicin sensitization. To substantiate this idea, we identified a TMPK inhibitor, YMU1. We found that YMU1 increases doxorubicin sensitivity in a variety of tumor cells. The mice therapy experiments also prove that YMU1 in conjunction with sublethal dose of doxorubicin greatly suppresses tumor growth. Most importantly, YMU1 on its own did not produce genotoxic effects in cells or mice. Although TS inhibitors and other nucleotide metabolite blockers have also been used as chemosensitizers (Garg et al., 2010), it should be emphasized that these anticancer agents are toxic to the genomic DNA in normal cycling cells as well. Their therapeutic effect stems solely from their ability to cause extensive DNA damage by which they produce nonspecific toxicity. We propose that the therapeutic advantage of a TMPK inhibitor over these conventional compounds is the fact that it shows a specific toxicity toward malignant cells that contain DNA lesions with increased levels of R2 expression. Here, we proposed that YMU1 is a promising lead compound for the development of a very mild chemosensitization regimen that primes tumor cells and makes them sensitive to sublethal doses of doxorubicin; the result should involve lethality that targets these tumor cells while causing minimal side effects with respect to normal cycling cells.

EXPERIMENTAL PROCEDURES

Chemistry

Compound YMU1, ethyl 4-(2-(4,6-dimethyl-3-oxoisothiazolo[5,4-b]pyridin-2(3H)-yl)acetyl)piperazine-1-carboxylate, was synthesized using 2-chloro-4,6-dimethylnicotinonitrile as a starting material. See Supplemental Experimental Procedures for synthetic schemes and procedures; additional characterization data are available upon request.

Homologous Recombination Assay

U2OS DR-GFP cells with the integrated homologous recombination reporter DR-GFP (Pierce et al., 1999) were transfected with TMPK siRNA, which was followed by transfection with the I-SceI expression vector (pCBA-I-SceI) for 48 hr. The recombination efficiency was examined by flow cytometric analysis of the frequency of GFP^+ cells.

In Vivo Chemotherapy

All mice experiments were approved by the biosafety committee of National Yang-Ming University and conformed to the national guidelines and regulations. Female BALB/c AnN.Cg-Foxnl^{nu}/Crl Nurl mice 6–8 weeks of age (National Laboratory Animal Center, Taiwan) were used for the tumor xenograft model. HCT-116 $p53^{-/-}$ cells (1×10^6) were subcutaneously implanted in the right flank of each mouse. Treatment began when the tumor size was about 1 mm^3. Mice (n = 32) were randomly allocated to four groups, namely vehicle (15% TEG), doxorubicin (1.25 mg/kg twice a week), YMU1 (5 mg/kg thrice a week), and YMU (5 mg/kg thrice a week) combined with doxorubicin (1.25 mg/kg twice a week). Mice were administered with the indicated treatment by intraperitoneal injection for four weeks, after which the mice were kept in a drug-free condition for additional two weeks. The tumor size was measured every day after the initiation of drug treatment by electronic caliper. Tumor volume = length (mm) × width^2 (mm^2) / 2.

Statistical Analyses

A two-tailed Student's t test was used to assess DNA lesions, tumor size, and tumor weight (*$p < 0.05$, **$p < 0.01$). Data are presented as mean ± SD. All other experimental procedures are described in the Supplemental Experimental Procedures.

SUPPLEMENTAL INFORMATION

Supplemental Information includes seven figures, one table, Supplemental Experimental Procedures, and Supplemental References and can be found with this article online at doi:10.1016/j.ccr.2012.04.038.

ACKNOWLEDGMENTS

We thank B. Vogelstein (The Johns Hopkins University Medical Institutions), M.B. Kastan (St. Jude Children's Research Hospital, Memphis), A.J. Pierce (University of Kentucky, Lexington), S.Y. Shieh (Institute of Biomedical Sciences, Academia Sinica, Taiwan), C.H. Lin (Institute of Biological Chemistry, Academia Sinica, Taiwan), W.H. Lee (Department of Biological Chemistry University of California, Irvine USA), C.L. Hsieh (Graduate Institute of Cancer Biology, China Medical University Hospital, Taiwan), and O.K. Lee (Stem Cell Research Center, National Yang-Ming University, Taiwan) for providing $p53^{+/+}$, $p53^{-/-}$ HCT-116 cell lines, I-PpoI, the I-SceI expression vectors, the U2OS stably expressing DR-GFP reporter, Capan-1, HCC1937, MCF-10A H184B5F5/M10, HRCE, and HBMSC, respectively. The authors are indebted to Y.J. Lee, P.S. Jiang, and T.Y. Huang at National Yang-Ming University for their technical assistance and P.-Y. Lin (Mass spectrometry facility, Academia Sinica, Taiwan) for her help in mass spectrum analysis. We are also grateful to C.H. Wong and Y.T. Wu (Genome Center, Academia Sinica) for generously providing the chemical library and technical support. This study was supported by grants NHRI-EX-100-10005NI from National Health Research Institute and NSC 100-2325-B-010-001 from National Science Council, Taiwan, and a grant from Aim for the Top University plan in National Yang-Ming University supported by the Ministry of Education, Taiwan.

Received: August 23, 2011
Revised: January 3, 2012
Accepted: April 24, 2012
Published: July 9, 2012

REFERENCES

Ahmad, S.I., Kirk, S.H., and Eisenstark, A. (1998). Thymine metabolism and thymineless death in prokaryotes and eukaryotes. Annu. Rev. Microbiol. *52*, 591–625.

Berkovich, E., Monnat, R.J., Jr., and Kastan, M.B. (2007). Roles of ATM and NBS1 in chromatin structure modulation and DNA double-strand break repair. Nat. Cell Biol. *9*, 683–690.

Bessman, M.J., Lehman, I.R., Adler, J., Zimmerman, S.B., Simms, E.S., and Kornberg, A. (1958). Enzymatic synthesis of deoxyribonucleic acid. III. The incorporation of pyrimidine and purine analogues into deoxyribonucleic acid. Proc. Natl. Acad. Sci. USA *44*, 633–640.

(E) After 2 weeks recovered from treatment, the mice were sacrificed to allow tumor weight measurement. All error bars in (D) and (E) represent SEM (n = 8).
(F) Ki 67 proliferation marker staining of a tumor is shown in the lower panel (scale bar, 50 μm).
(G) Model of doxorubicin sensitization by YMU1 in malignant cancer cells. Both R2/R1 and TMPK are recruited to the site of doxorubicin-induced double-strand breaks, where dATP, dGTP, dCTP, dTTP, and dUTP are synthesized in a site-specific manner. Inhibition of TMPK decreases dTTP formation at the DNA damage sites, which causes futile DNA repair due to dUTP incorporation.
See also Figure S7 and Table S1.

Burkhalter, M.D., Roberts, S.A., Havener, J.M., and Ramsden, D.A. (2009). Activity of ribonucleotide reductase helps determine how cells repair DNA double strand breaks. DNA Repair (Amst.) *8*, 1258–1263.

Caldecott, K.W. (2008). Single-strand break repair and genetic disease. Nat. Rev. Genet. *9*, 619–631.

Chabes, A., and Stillman, B. (2007). Constitutively high dNTP concentration inhibits cell cycle progression and the DNA damage checkpoint in yeast *Saccharomyces cerevisiae*. Proc. Natl. Acad. Sci. USA *104*, 1183–1188.

Chabes, A.L., Pfleger, C.M., Kirschner, M.W., and Thelander, L. (2003). Mouse ribonucleotide reductase R2 protein: a new target for anaphase-promoting complex-Cdh1-mediated proteolysis. Proc. Natl. Acad. Sci. USA *100*, 3925–3929.

Engström, Y., Eriksson, S., Jildevik, I., Skog, S., Thelander, L., and Tribukait, B. (1985). Cell cycle-dependent expression of mammalian ribonucleotide reductase: differential regulation of the two subunits. J. Biol. Chem. *260*, 9114–9116.

Fan, H., Villegas, C., Huang, A., and Wright, J.A. (1998). The mammalian ribonucleotide reductase R2 component cooperates with a variety of oncogenes in mechanisms of cellular transformation. Cancer Res. *58*, 1650–1653.

Flick, K.E., Jurica, M.S., Monnat, R.J., Jr., and Stoddard, B.L. (1998). DNA binding and cleavage by the nuclear intron-encoded homing endonuclease I-PpoI. Nature *394*, 96–101.

Garg, D., Henrich, S., Salo-Ahen, O.M., Myllykallio, H., Costi, M.P., and Wade, R.C. (2010). Novel approaches for targeting thymidylate synthase to overcome the resistance and toxicity of anticancer drugs. J. Med. Chem. *53*, 6539–6549.

Håkansson, P., Hofer, A., and Thelander, L. (2006). Regulation of mammalian ribonucleotide reduction and dNTP pools after DNA damage and in resting cells. J. Biol. Chem. *281*, 7834–7841.

Hartlerode, A.J., and Scully, R. (2009). Mechanisms of double-strand break repair in somatic mammalian cells. Biochem. J. *423*, 157–168.

Holthausen, J.T., Wyman, C., and Kanaar, R. (2010). Regulation of DNA strand exchange in homologous recombination. DNA Repair (Amst.) *9*, 1264–1272.

Hu, C.M., and Chang, Z.F. (2008). Synthetic lethality by lentiviral short hairpin RNA silencing of thymidylate kinase and doxorubicin in colon cancer cells regardless of the p53 status. Cancer Res. *68*, 2831–2840.

Hu, C.M., and Chang, Z.F. (2010). A bioluminescent method for measuring thymidylate kinase activity suitable for high-throughput screening of inhibitor. Anal. Biochem. *398*, 269–271.

Jensen, R.A., Page, D.L., and Holt, J.T. (1994). Identification of genes expressed in premalignant breast disease by microscopy-directed cloning. Proc. Natl. Acad. Sci. USA *91*, 9257–9261.

Kastan, M.B., and Bartek, J. (2004). Cell-cycle checkpoints and cancer. Nature *432*, 316–323.

Katada, H., Harumoto, T., Shigi, N., and Komiyama, M. (2012). Chemical and biological approaches to improve the efficiency of homologous recombination in human cells mediated by artificial restriction DNA cutter. Nucleic Acids Res. *40*, e81.

Krokan, H.E., Drabløs, F., and Slupphaug, G. (2002). Uracil in DNA—occurrence, consequences and repair. Oncogene *21*, 8935–8948.

Ladner, R.D., and Caradonna, S.J. (1997). The human dUTPase gene encodes both nuclear and mitochondrial isoforms: differential expression of the isoforms and characterization of a cDNA encoding the mitochondrial species. J. Biol. Chem. *272*, 19072–19080.

Lieber, M.R. (2010). The mechanism of double-strand DNA break repair by the nonhomologous DNA end-joining pathway. Annu. Rev. Biochem. *79*, 181–211.

Liu, X., Lai, L., Wang, X., Xue, L., Leora, S., Wu, J., Hu, S., Zhang, K., Kuo, M.L., Zhou, L., et al. (2011). Ribonucleotide reductase small subunit M2B prognoses better survival in colorectal cancer. Cancer Res. *71*, 3202–3213.

Longley, D.B., Harkin, D.P., and Johnston, P.G. (2003). 5-fluorouracil: mechanisms of action and clinical strategies. Nat. Rev. Cancer *3*, 330–338.

Mah, L.J., El-Osta, A., and Karagiannis, T.C. (2010). gammaH2AX: a sensitive molecular marker of DNA damage and repair. Leukemia *24*, 679–686.

Mathews, C.K. (2006). DNA precursor metabolism and genomic stability. FASEB J. *20*, 1300–1314.

McIntosh, E.M., Ager, D.D., Gadsden, M.H., and Haynes, R.H. (1992). Human dUTP pyrophosphatase: cDNA sequence and potential biological importance of the enzyme. Proc. Natl. Acad. Sci. USA *89*, 8020–8024.

Mimitou, E.P., and Symington, L.S. (2009). DNA end resection: many nucleases make light work. DNA Repair (Amst.) *8*, 983–995.

Moss, J., Tinline-Purvis, H., Walker, C.A., Folkes, L.K., Stratford, M.R., Hayles, J., Hoe, K.L., Kim, D.U., Park, H.O., Kearsey, S.E., et al. (2010). Break-induced ATR and Ddb1-Cul4(Cdt)^2 ubiquitin ligase-dependent nucleotide synthesis promotes homologous recombination repair in fission yeast. Genes Dev. *24*, 2705–2716.

Nagaraju, G., and Scully, R. (2007). Minding the gap: the underground functions of BRCA1 and BRCA2 at stalled replication forks. DNA Repair (Amst.) *6*, 1018–1031.

Niida, H., Katsuno, Y., Sengoku, M., Shimada, M., Yukawa, M., Ikura, M., Ikura, T., Kohno, K., Shima, H., Suzuki, H., et al. (2010a). Essential role of Tip60-dependent recruitment of ribonucleotide reductase at DNA damage sites in DNA repair during G1 phase. Genes Dev. *24*, 333–338.

Niida, H., Shimada, M., Murakami, H., and Nakanishi, M. (2010b). Mechanisms of dNTP supply that play an essential role in maintaining genome integrity in eukaryotic cells. Cancer Sci. *101*, 2505–2509.

Nordlund, P., and Reichard, P. (2006). Ribonucleotide reductases. Annu. Rev. Biochem. *75*, 681–706.

Pierce, A.J., Johnson, R.D., Thompson, L.H., and Jasin, M. (1999). XRCC3 promotes homology-directed repair of DNA damage in mammalian cells. Genes Dev. *13*, 2633–2638.

Pontarin, G., Ferraro, P., Rampazzo, C., Kollberg, G., Holme, E., Reichard, P., and Bianchi, V. (2011). Deoxyribonucleotide metabolism in cycling and resting human fibroblasts with a missense mutation in p53R2, a subunit of ribonucleotide reductase. J. Biol. Chem. *286*, 11132–11140.

Powell, S.N., and Kachnic, L.A. (2003). Roles of BRCA1 and BRCA2 in homologous recombination, DNA replication fidelity and the cellular response to ionizing radiation. Oncogene *22*, 5784–5791.

Reichard, P. (1988). Interactions between deoxyribonucleotide and DNA synthesis. Annu. Rev. Biochem. *57*, 349–374.

Robert, T., Vanoli, F., Chiolo, I., Shubassi, G., Bernstein, K.A., Rothstein, R., Botrugno, O.A., Parazzoli, D., Oldani, A., Minucci, S., and Foiani, M. (2011). HDACs link the DNA damage response, processing of double-strand breaks and autophagy. Nature *471*, 74–79.

San Filippo, J., Sung, P., and Klein, H. (2008). Mechanism of eukaryotic homologous recombination. Annu. Rev. Biochem. *77*, 229–257.

Shao, J., Zhou, B., Zhu, L., Qiu, W., Yuan, Y.C., Xi, B., and Yen, Y. (2004). In vitro characterization of enzymatic properties and inhibition of the p53R2 subunit of human ribonucleotide reductase. Cancer Res. *64*, 1–6.

Shao, J., Zhou, B., Chu, B., and Yen, Y. (2006). Ribonucleotide reductase inhibitors and future drug design. Curr. Cancer Drug Targets *6*, 409–431.

Traut, T.W. (1994). Physiological concentrations of purines and pyrimidines. Mol. Cell. Biochem. *140*, 1–22.

Xu, X., Page, J.L., Surtees, J.A., Liu, H., Lagedrost, S., Lu, Y., Bronson, R., Alani, E., Nikitin, A.Y., and Weiss, R.S. (2008). Broad overexpression of ribonucleotide reductase genes in mice specifically induces lung neoplasms. Cancer Res. *68*, 2652–2660.

Yanamoto, S., Kawasaki, G., Yoshitomi, I., and Mizuno, A. (2003). Expression of p53R2, newly p53 target in oral normal epithelium, epithelial dysplasia and squamous cell carcinoma. Cancer Lett. *190*, 233–243.

Zhang, K., Hu, S., Wu, J., Chen, L., Lu, J., Wang, X., Liu, X., Zhou, B., and Yen, Y. (2009). Overexpression of RRM2 decreases thrombspondin-1 and increases VEGF production in human cancer cells in vitro and in vivo: implication of RRM2 in angiogenesis. Mol. Cancer *8*, 11.